

---

# Depth-Breadth Synergy in RLVR: Unlocking LLM Reasoning Gains with Adaptive Exploration

---

Zhicheng Yang<sup>1</sup> Zhijiang Guo<sup>1,2</sup> Yinya Huang<sup>3</sup> Yongxin Wang<sup>4</sup> Dongchun Xie<sup>5</sup> Hanhui Li<sup>5</sup> Yiwei Wang<sup>6</sup>  
Xiaodan Liang<sup>4,5</sup> Jing Tang<sup>1,2</sup>

yangzhch6@gmail

Project Repo: <https://github.com/yangzhch6/DARS>

## Abstract

Reinforcement Learning with Verifiable Reward (RLVR) is a powerful method for enhancing the reasoning abilities of Large Language Models, but its full potential is limited by a lack of exploration in two key areas: **Depth** (the difficulty of problems) and **Breadth** (the number of training instances). Our analysis of the popular GRPO algorithm reveals a bias that down-weights difficult, low-accuracy problems, which are crucial for improving reasoning skills. To address this, we introduce **Difficulty Adaptive Rollout Sampling (DARS)**, a method that re-weights difficult problems by using targeted, multi-stage rollouts. DARS increases the number of rollout outcomes for these harder problems according to our proposed re-balancing schedules and leads to consistent gains in *Pass@K*. We discovered that increasing rollout size alone does not improve performance and may actually impair it. In contrast, scaling the batch size to increase breadth via full-batch updates significantly boosted *Pass@1* metrics. This improvement stems from higher token-level entropy, ensuring robust exploration and minimized gradient noise. Finally, we present DARS-Breadth, a combined approach that uses DARS with a large breadth of training data. This method demonstrates simultaneous gains in both *Pass@K* and *Pass@1*, confirming that depth (adaptive exploration) and breadth (scaling the training data) are orthogonal and essential dimensions for unlocking the full power of RLVR.

## 1. Introduction

The emergence of reasoning-centric Large Language Models (LLMs) exemplified by OpenAI-o1 (Jaech et al., 2024), DeepSeek-R1 (Guo et al., 2025), and Kimi-1.5 (Team et al., 2025), has pushed the frontier of LLM capability,

<sup>1</sup>HKUST-GZ <sup>2</sup>HKUST <sup>3</sup>ETH AI Center, ETH Zurich  
<sup>4</sup>MBZUAI <sup>5</sup>Sun Yat-Sen University <sup>6</sup>University of California, Merced.

especially for demanding tasks in complex reasoning such as mathematics and programming. Unlike conventional instruction tuning that relies on human-labeled data or RLHF pipelines that demand an auxiliary, well-trained reward model (Ouyang et al., 2022b; Achiam et al., 2023; Grattafiori et al., 2024), this leap is driven by large-scale Reinforcement Learning with Verifiable Rewards (RLVR; Guo et al. 2025; Zeng et al. 2025) for which correctness can be automatically and deterministically checked. The rewards of RLVR are granted solely when a model’s output matches the ground-truth mathematical answer or passes all unit tests for code, allowing scalable verification without manual labeling. RLVR is now regarded as a promising path toward self-evolving LLMs, potentially bringing us closer to more powerful intelligence.

However, existing RLVR frameworks inadequately address the interplay between exploration depth (difficulty scaling) and breadth (iteration instance quantity scaling), which leads to insufficient performance gain for both *Pass@1* and *Pass@K*. In this paper, we conduct a systematic analysis of these two under-exploited dimensions in RLVR.

For the dimension of **depth**, our investigation reveals that existing methods of GRPO (Shao et al., 2024) and its variants (Yu et al., 2025; Liu et al., 2025b), while adept at estimating the advantage of a single rollout, are undermined by a distorted cumulative advantage at the group level. This distortion disproportionately allocates attention to instances of medium difficulty, neglecting high-difficulty instances indispensable for complex reasoning, as illustrated in Figure 1. This bias fundamentally limits depth, the hardest problems a model can learn to solve, and constrains *Pass@K* performance. To counteract this depth neglect, we propose Difficulty-Adaptive Rollout Sampling (**DARS**). DARS performs a lightweight first-stage rollout to estimate per-problem accuracies, then allocates additional compute via targeted multi-stage rollouts to low-accuracy problems. By expanding sampling on hard problems, DARS re-weights the cumulative advantage, making it easier for LLMs to learn ‘deep’ samples and improving *Pass@K* performance.

We further identify **breadth** as the instance quantity consumed in a single iteration. We observe that breadth has a significant impact on the LLM’s performance and con-

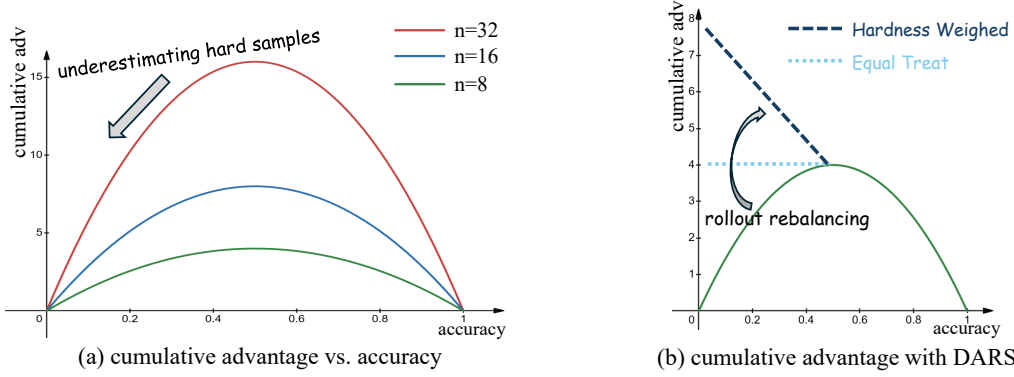


Figure 1. Statistical results of cumulative advantage. Group relative advantage calculation methods underestimate high-difficulty problems.  $n$  denotes group size.

tinuous exploration capability, as shown in Figure 4. We significantly increase the training batch size and replace PPO-minibatch updates with full-batch updates for multiple PPO-epochs. This seemingly simple change dramatically improves  $Pass@1$  and sustains high token-level entropy throughout training, suggesting that breadth acts as implicit entropy regularization that delays premature convergence. Importantly, the gains from breadth are complementary to those from depth: we present **DARS-Breadth** that combines our DARS with large-breadth training, producing simultaneous boosts in both  $Pass@K$  and  $Pass@1$ . Our contributions can be summarized as follows:

- We conduct a systematic analysis on depth and breadth in RLVR, and uncover the depth bias in GRPO: cumulative advantage underweights low-accuracy, high-difficulty samples, capping  $Pass@K$  performance.
- We introduce DARS, which reallocates compute to the hard problems via multi-stage rollout sampling. DARS reweights the cumulative advantage distribution and quantitatively expands the sparse reward signals for difficult problems. In practice, DARS significantly improves  $Pass@K$  performance. We elaborate on the impact of cumulative advantage on the gradient norm in Appendix B.2, and further discuss the relationship between DARS-HW and MaxRL (Tajwar et al., 2026) in Appendix C.
- We further illustrate that large breadth matters for the  $Pass@1$  performance. Moreover, by combining DARS with large breadth training, we reveal the complementarity of Depth and Breadth in RLVR and acquire simultaneous boosts in both  $Pass@K$  and  $Pass@1$  performance.

## 2. Understanding RLVR from Depth and Breadth

### 2.1. Depth: The Hardest Problem Sampled in RLVR

We first identify **Depth** as the hardest problem that can be correctly answered in the RLVR training process. In the GRPO training process, groups whose entire rollouts yield

incorrect answers suffer from gradient vanishing. Hence, sampling high-difficulty questions with correct reasoning paths is crucial for LLM training. We first show that merely increasing rollout size does not consistently yield significant gains in  $Pass@K$  performance, and sometimes can even be harmful. We then quantify GRPO’s cumulative advantage and highlight its under-weighting of high-difficulty samples.

**Naive Scaling of Rollout Size Benefits  $Pass@1$ , But Not Necessarily  $Pass@K$ .** We present the training dynamics of  $Pass@1$  and  $Pass@K$  performance during the RLVR training process in Figure 2. Enlarging the rollout size allows the sampling of correct solutions to hard problems during training. We originally assumed this would benefit  $Pass@K$  performance; however, experimental results show that this is not always the case. We find that Qwen2.5-Math-7B can significantly benefit from an increased rollout size, whereas for Qwen2.5-Math-1.5b, naively scaling rollout size can even harm  $Pass@K$  performance.

**Cumulative Advantage Bias in GRPO Variants hinders the improvement of  $Pass@K$ .** In the GRPO framework, the advantage estimation is derived by normalizing binary rewards:

$$\hat{A}_i^{std} = \frac{r_i - u}{\sigma}, \quad \hat{A}_i^{nostd} = r_i - u, \quad (1)$$

where  $r_i$  is the binary reward of  $i_{th}$  rollout,  $u$  is the mean value of the group rewards  $u = \text{mean}(\{R_i\}_{i=1}^G)$  and  $\sigma$  is the standard deviation of the group rewards  $\sigma = \text{std}(\{R_i\}_{i=1}^G)$ . In the case of binary rewards,  $u$  also represents the accuracy of LLM rollouts. Dr. GRPO (Liu et al., 2025b) removes the standard-deviation term from the advantage computation to eliminate question-level difficulty bias, and demonstrates its superiority through extensive experiments. Consequently, the experiments reported in this study were conducted primarily through the Dr. GRPO methodology. We show more results of std-based advantage in Appendix D.

For a group  $G$  with rollout size  $N$ , we define the **cumulative advantage** of a group as the sum of the absolute values of

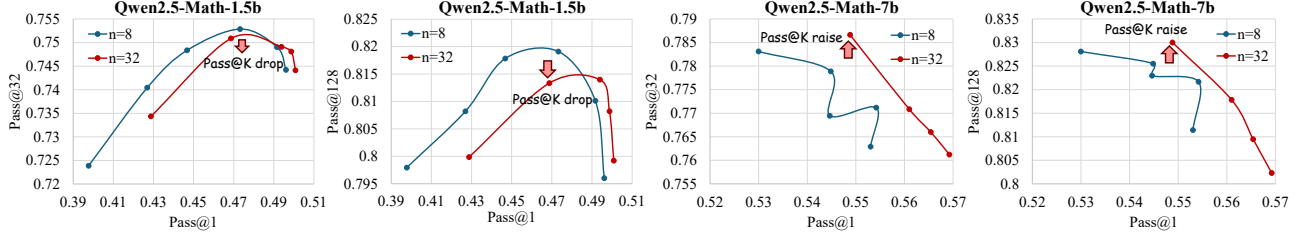


Figure 2. Training dynamics of  $Pass@1$  and  $Pass@K$  performance of Qwen2.5-Math-1.5B and -7B with different rollout size.

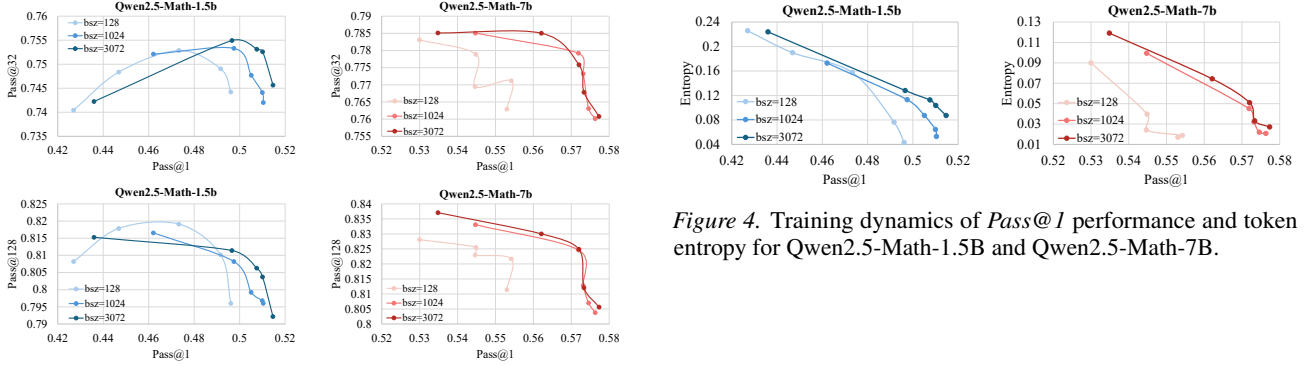


Figure 3. Training dynamics of  $Pass@1$  and  $Pass@K$  performance of Qwen2.5-Math-1.5B and -7B with different batch size.

sample advantages:  $\mathcal{A}_{\text{group}} = \sum_{i=1}^G |\hat{A}_i|$ . The cumulative advantage reflects how much the algorithm weights each sample. Specifically, for Dr. GRPO,

$$\mathcal{A}_{\text{group}} = 2Nu(1 - u). \quad (2)$$

The cumulative advantage functional curve is plotted in Figure 1. As shown in the figure, group-based advantage computation funnels its weight toward problems of medium difficulty while largely overlooking those that are highly difficult. This bias limits the  $Pass@K$  performance of RLVR.

## 2.2. Breadth: Iteration Instance Quantity in RLVR

We define **Breadth** as the number of instances used per iteration of the RLVR process. We’ll show how increasing the batch size for the RLVR process improves the  $Pass@1$  performance.

**Breadth Matters for  $Pass@1$  Performance.** Most studies (Liu et al., 2025b;a; Yan et al., 2025; Fu et al., 2025) conventionally set the batch size to 128. In this subsection, we drastically increase the batch size to 3072 and plot the training dynamics of  $Pass@1$  and  $Pass@32$  performance in Figure 3. Naively increasing the batch size brings a  $Pass@1$  improvement for all models, yet it harms the  $Pass@128$  performance of Qwen2.5-Math-1.5B. We consider that increasing the quantity of instances used in each iteration makes the gradient direction more accurate and reduces the

impact of noise, thereby improving  $Pass@1$  performance.

## Breadth Sustains Entropy for Model Exploration.

High token entropy in LLMs indicates strong exploration capabilities. Our analysis shows a relationship between  $Pass@1$  and token entropy during training. As illustrated in Figure 4, increased training breadth enables LLMs to achieve higher entropy at a given  $Pass@1$  accuracy. We believe a large training breadth acts as a form of entropy regularization, preventing premature convergence and boosting  $Pass@1$  performance while maintaining high entropy.

## 3. Methodology

In Section 2, we analyze the bias inherent in group-based advantage computation. To solve this issue, we introduce Difficulty Adaptive Rollout Sampling (**DARS**), which rebalances the cumulative advantage via multi-stage sampling. By further synergizing the depth and breadth training dimensions, we propose DARS-B, which improves both  $Pass@1$  and  $Pass@K$ .

### 3.1. Difficulty Adaptive Rollout Sampling (DARS)

As shown in Figure 5, given a data batch  $\mathcal{B} = \{q_j\}_{j=1}^M$  of reasoning questions, DARS operates in two phases: (i) **pre-rollout difficulty estimation** that assigns to each question  $q_j$  a scalar difficulty score  $x_j \in [0, 1]$ ; and (ii) **multi-stage rollout re-balancing** that dynamically decides how many additional trajectories  $\Delta n_j$  shall be allocated to  $q_j$  so that the cumulative advantage for low-accuracy problems is up-weighted. To simplify the subsequent formula

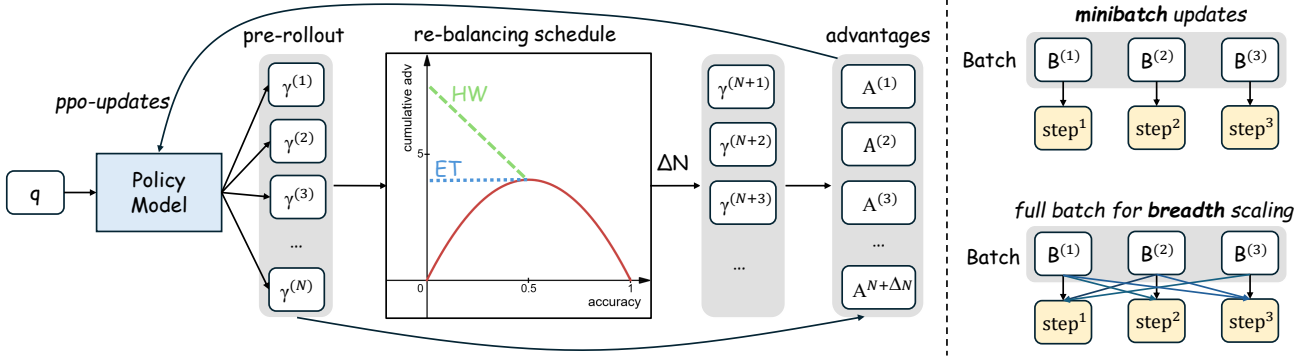


Figure 5. The overall training framework of our Difficulty Adaptive Rollout Sampling (**DARS**) with breadth scaling. Our DARS consists of 2 phases: 1) a pre-rollout stage to evaluate the difficulty of the given question, and 2) a re-balancing rollout stage to adjust the cumulative advantage. For breadth scaling, we replace PPO minibatch as full batch with multiple PPO epochs.

representation, we define

$$\mathcal{S}(\hat{a}_j) = 2\hat{a}_j(1 - \hat{a}_j). \quad (3)$$

**Phase 1: Pre-Rollout Difficulty Estimation.** For every  $q_j$ , we draw a light first-stage rollout consisting of  $N^{pre}$  independent trajectories  $\{\tau_j^{(i)}\}$ . Let the per-trajectory reward be binary,  $r_j^{(i)} \in \{0, 1\}$ . We define the empirical accuracy

$$\hat{a}_j = \frac{1}{N^{pre}} \sum_{i=1}^{N^{pre}} r_j^{(i)}. \quad (4)$$

The difficulty score is then set to the complementary accuracy  $x_j = 1 - \hat{a}_j$ , so that  $x_j \approx 1$  for the hardest problems and  $x_j \approx 0$  for the easiest ones.

**Phase 2: Multi-Stage Rollout Re-Balancing.** Let  $\mathcal{A}_{\text{group}}^N(u)$  denote the cumulative advantage under GRPO for a group whose average accuracy is  $u$  with rollout size  $N$ . We aim to reallocate  $\Delta N$  additional trajectories across the mini-batch so that the **effective** cumulative advantage for each question becomes an increasing function of its difficulty. To control the computing cost, we cap the rollout sampling upper limit at  $N^{\max}$ . To this end, we design two rebalancing schedules.

**Schedule 1: Equal-Treatment (ET).** For every question  $q_j$  we enforce the rebalanced cumulative advantage as:

$$\mathcal{A}_{\text{group}}^{ET}(q_j) = \mathcal{A}_{\text{group}}^{N^{pre}}(0.5). \quad (5)$$

We raise the cumulative advantage of all difficulty problems ( $\hat{a}_j < 0.5$ ) to the level achieved by a medium-difficulty problem with accuracy  $\hat{a}_j = 0.5$ . The required extra trajectories are

$$\Delta n_j^{ET} = \min\left(\left\lceil \frac{\mathcal{A}_{\text{group}}^{N^{pre}}(0.5) - \mathcal{A}_{\text{group}}^{N^{pre}}(\hat{a}_j)}{\mathcal{S}(\hat{a}_j)} \right\rceil, N^{\max} - N^{pre}\right). \quad (6)$$

**Schedule 2: Hardness-Weighted (HW).** We now impose a monotonically increasing re-weighting that allocates more rollouts to lower-accuracy problems:

$$\mathcal{A}_{\text{group}}^{HW}(q_j) = 2(1 - x_j)\mathcal{A}_{\text{group}}^{N^{pre}}(0.5). \quad (7)$$

This yields

$$\Delta n_j^{HW} = \min\left(\left\lceil \frac{2x_j \cdot \mathcal{A}_{\text{group}}^{N^{pre}}(0.5) - \mathcal{A}_{\text{group}}^{N^{pre}}(\hat{a}_j)}{\mathcal{S}(\hat{a}_j)} \right\rceil, N^{\max} - N^{pre}\right). \quad (8)$$

### 3.2. Depth Synergy with Breadth Scaling

Our analysis in Section 2.2 empirically confirms the substantial *Pass@1* improvements from large-breadth training. While DARS primarily optimizes training depth via multi-stage rollout rebalance, its dynamic batch-size adjustments preclude standard PPO-style mini-batch updates. To resolve this architectural constraint while leveraging breadth benefits, we replace PPO’s mini-batch updates with full-batch gradient descent across multiple PPO epochs, as illustrated in Figure 5. This modification ensures compatibility with DARS’s dynamic allocation while maximizing effective training breadth per optimization step. We term this integrated approach **DARS-Breadth**, unifying depth-adaptive sampling with breadth maximization.

Full-batch training offers two key advantages: (1) elimination of mini-batch gradient noise, and (2) sustained token-level exploration, acting as implicit regularization against premature convergence. The resulting framework demonstrates complementary gains—DARS improves *Pass@K* through depth optimization, while large-breadth training enhances *Pass@1*, highlighting their synergistic roles in RLVR optimization.

Table 1. Overall performance of  $Pass@1$  (Avg@128) and  $Pass@128$  of Qwen2.5-Math series.

Base Model + Method	AIME24	MATH500	Olympiad	AMC	Minerva	Avg@128	Pass@128
Qwen2.5-Math-1.5B	4.0	35.1	16.2	20.8	9.5	21.1	77.9
RLVR baseline	14.7	75.9	39.4	47.5	31.2	49.6	79.6
Depth-Naive	16.5	76.2	39.9	47.9	30.9	50.1	79.9
Breadth-Naive	18.5	77.6	41.7	49.8	<b>31.9</b>	51.5	79.2
<b>DARS-1.5B-ET</b>	15.8	76.0	40.9	47.2	30.0	50.0	81.2
<b>DARS-1.5B-ET-Breadth</b>	<u>18.6</u>	<b>79.4</b>	<b>42.9</b>	<u>50.6</u>	<u>31.7</u>	<b>52.5</b>	80.8
<b>DARS-1.5B-HW</b>	17.7	76.4	40.0	48.4	30.8	50.0	<u>82.1</u>
<b>DARS-1.5B-HW-Breadth</b>	<b>19.3</b>	<u>79.0</u>	<u>42.7</u>	<b>51.9</b>	31.6	<u>52.4</u>	<b>82.2</b>
Qwen2.5-Math-7B	11.6	52.3	19.7	35.2	15.3	30.1	82.1
RLVR baseline	26.8	82.2	44.3	57.2	35.7	55.3	81.4
Depth-Naive	28.0	83.8	46.4	59.0	37.3	57.0	80.3
Breadth-Naive	30.5	83.7	47.3	<u>61.4</u>	37.7	57.7	79.2
<b>DARS-7B-ET</b>	26.9	83.2	46.6	57.3	<b>38.5</b>	57.0	81.7
<b>DARS-7B-ET-Breadth</b>	<b>33.3</b>	<u>83.8</u>	<u>47.8</u>	61.3	<u>38.4</u>	<u>58.1</u>	82.1
<b>DARS-7B-HW</b>	30.1	83.5	47.1	59.4	37.2	57.3	<b>83.5</b>
<b>DARS-7B-HW-Breadth</b>	<u>33.0</u>	<b>84.5</b>	<b>48.4</b>	<b>63.0</b>	36.9	<b>58.4</b>	<u>83.4</u>

### 3.3. Training Target

We adopt the clipped objective of GRPO without the KL penalty term. Following Dr. GRPO, we likewise remove the response length handling from the GRPO target. Specifically, for a problem  $q$  sampled in training data  $\mathcal{D}$ , the training target is formalized as:

$$\mathcal{J}(\theta) = \mathbb{E}_{(q \sim \mathcal{D}, \{o_i\}_{i=1}^G \sim \pi_{\theta_{\text{old}}}(q))} \left[ \frac{1}{G} \sum_{i=1}^G \sum_{t=1}^{|o_i|} \left( \min \left( r_{i,t}(\theta) \hat{A}_{i,t}, \text{clip} \left( r_{i,t}(\theta), 1 - \varepsilon, 1 + \varepsilon \right) \hat{A}_{i,t} \right) \right) \right], \quad (9)$$

where

$$r_{i,t}(\theta) = \frac{\pi_{\theta}(o_{i,t} | q, o_{i,<t})}{\pi_{\theta_{\text{old}}}(o_{i,t} | q, o_{i,<t})}. \quad (10)$$

The token advantage  $\hat{A}_{i,t}$  is computed using Equation 1.

## 4. Experiments

### 4.1. Setup

**Evaluation and Training:** We evaluate the RLVR process using 5 widely used mathematical reasoning benchmarks: MATH-500 (Lightman et al., 2023), OlympiadBench (He et al., 2024), MinervaMath (Lewkowycz et al., 2022), AIME24, and AMC23. We combine all of the evaluation benchmarks to report  $Pass@1$  (Avg@128) and  $Pass@K$  performance. The training data used in this work is OpenR1-45K, which is a subset of OpenR1-Math-220k (Hugging Face, 2025). Moreover, we adopt the same unbiased, low-variance estimator for  $Pass@K$  as used in prior works (Yue et al., 2025a; Chen et al., 2021):

$$\text{pass}@K = \mathbb{E}_{x_i \sim \mathcal{D}} \left[ 1 - \frac{\binom{n-c_i}{k}}{\binom{n}{k}} \right].$$

Specifically, when  $K = N$ , the metric become:  $\text{pass}@K = c_1 \vee c_2 \vee \dots \vee c_{128}$ .

**Baseline and Methods:** We compare with: (1) *RLVR-baseline*: Dr. GRPO with rollout size 8 and batch size 128. (2) *Depth-Naive*: Simply increasing the rollout size to 32. (3) *Breadth-Naive*: Simply increasing the batch size to 3072. (4) *DARS-ET/HW*: Our algorithm introduced in Section 3.1 with Equal-Treat/Hardness-Weighted schedule, using batch size 128 and  $N^{\text{max}} = 32$ . (5) *DARS-ET/HW-Breadth*: Our Depth-and-Breadth synergy algorithm introduced in Section 3.2, using batch size 3072 and  $N^{\text{max}} = 32$ . For all methods, the number of PPO mini-steps is uniformly set to 2.

**Evaluation Protocol:** For all baselines, we select the checkpoint with the best  $Pass@1$  performance for reporting. For DARS, we selected the checkpoint that achieved the best  $Pass@128$  performance after surpassing the baseline  $Pass@1$  performance. Table 1 summarizes the Avg@128 performance on each benchmark, the overall  $Pass@1$  across all test data, and the  $Pass@128$  performance.

### 4.2. Main Results

Breadth scaling delivers a clear and consistent boost to Pass@1. Across every model scale and every benchmark, Breadth-Naive outperforms both the GRPO baseline and Depth-Naive, lifting average Pass@1 (Avg@128) by 1.9–3.7

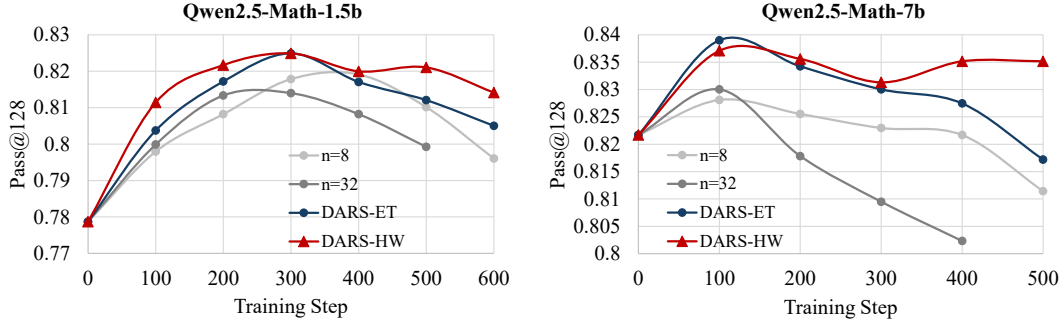


Figure 6. Training dynamics of  $Pass@128$  performance with different training steps of Qwen2.5-Math-1.5B and Qwen2.5-Math-7B.

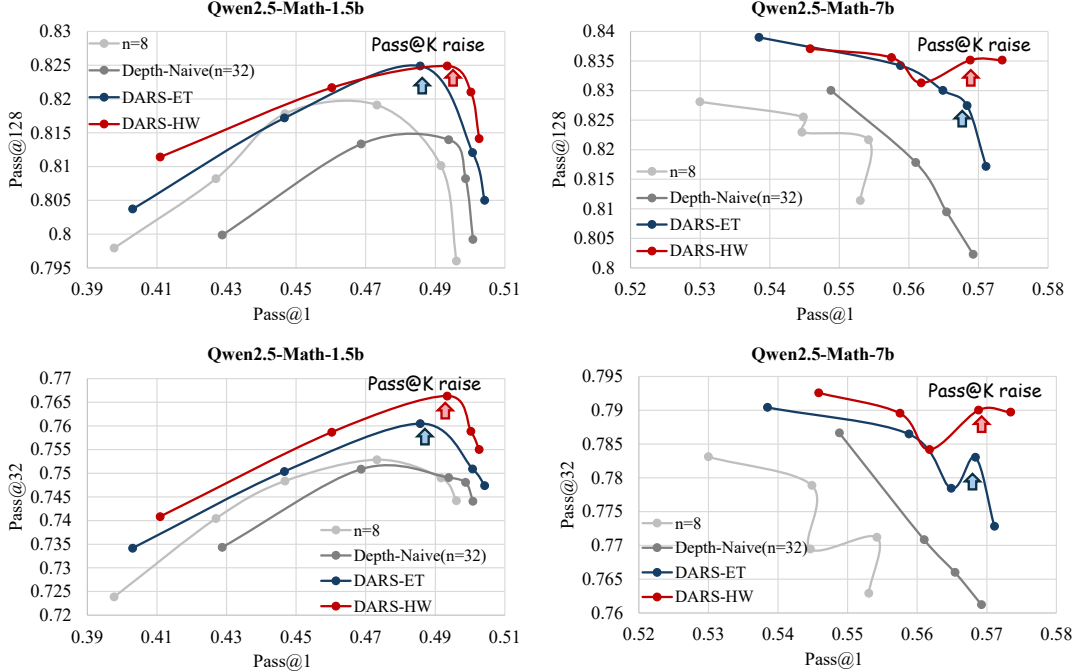


Figure 7. Training dynamics of  $Pass@32/Pass@128$  and  $Pass@1$  with different training steps of Qwen2.5-Math-1.5B and -7B.

points on AIME24, MATH500, and Olympiad tasks. This advantage is not merely additive: when breadth is combined with depth through DARS-Breadth, the margin widens further. DARS-Breadth reliably beats both Breadth-Naive and the original DARS variants, confirming our central hypothesis—depth and breadth are complementary, not competing, resources. Their synergy is what unlocks the next tier of LLM reasoning gains.

The practical impact is twofold. First, DARS-Breadth secures the highest  $Pass@1$ , the metric that matters most for single-shot deployment. Second, it matches the best  $Pass@128$  scores, demonstrating that the breadth-depth collaboration does not sacrifice the upper-bound capability revealed by heavy sampling. Finally, the choice of schedule matters: the HW schedule consistently yields superior  $Pass@K$  curves for both breadth and non-breadth training, while maintaining  $Pass@1$  parity with the ET schedule,

Table 2. Average rollout numbers per prompt.

Model	Naive	DARS-ET	DARS-HW
Qwen2.5-Math-1.5B	32	15.2 ( $\downarrow 52.5\%$ )	23.9 ( $\downarrow 25.3\%$ )
Qwen2.5-Math-7B	32	12.8 ( $\downarrow 60.0\%$ )	20.1 ( $\downarrow 37.2\%$ )

making it the preferred option across the board.

### 4.3. Training Dynamics and Ablation Study

In this subsection, we further show more training dynamics to illustrate properties of existing RLVR methods and the superiority of our DARS and DARS-B.

**$Pass@128$  performance surpasses the base model, peaks quickly, and then declines.** We conduct RLVR experiments with rollout size 8/32 to compare our DARS (with

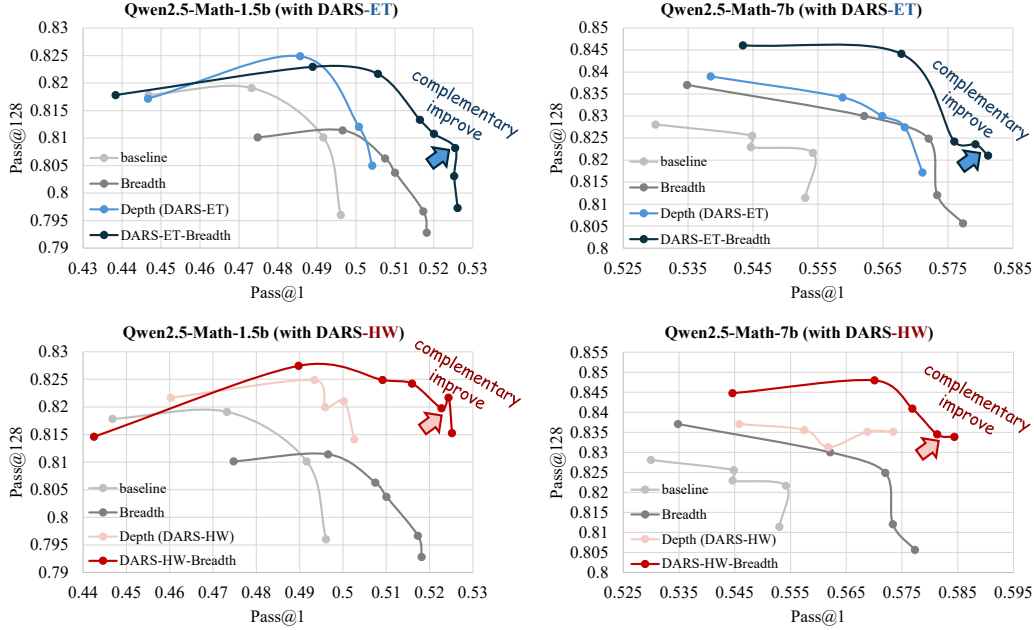


Figure 8. Depth and Breadth Synergy for  $Pass@1$  and  $Pass@K$  ( $K=128$ ) performance.

Table 3. Overall performance of  $Pass@1$  (Avg@128) and  $Pass@128$  performance of Llama-3.1-8B.

Base Model + Method	AIME24	MATH500	Olympiad	AMC	Minerva	Avg@128	Pass@128
Llama-3.1-8B	0.23	6.13	1.54	2.76	2.72	3.25	52.7
GRPO baseline	0.66	29.6	7.09	10.1	15.7	15.8	56.5
Depth-Naive	0.43	33.6	9.40	12.3	19.7	18.9	58.6
Breadth-Naive	0.79	34.4	9.34	12.2	19.0	19.0	61.1
<b>DARS-Llama-ET-Breadth</b>	<b>1.46</b>	<b>39.4</b>	<b>12.0</b>	<b>13.2</b>	<b>20.1</b>	<b>22.0</b>	<b>67.2</b>
<b>DARS-Llama-HW-Breadth</b>	<b>1.11</b>	<b>39.0</b>	<b>12.0</b>	<b>13.3</b>	<b>19.8</b>	<b>21.8</b>	<b>68.7</b>

$N^{\max} = 32$ ), the training dynamics of  $Pass@128$  performance during training is shown in Figure 6. Across all settings,  $Pass@128$  surpasses the base model during training, but declines after peaking, indicating that over-training with RLVR harms  $Pass@128$  performance. Notably, DARS (with  $N^{\max} = 32$ ) incurs substantially less inference cost than naively scaling the rollout size to  $n = 32$ . Despite this being an unfair comparison in terms of computational expenditure, our DARS not only attains the highest peak  $Pass@128$  performance but also outperforms all other settings.

**Depth Training with DARS Improve  $Pass@K$  Performance and Training Efficiency.** Because the  $Pass@K$  ( $K=32/128$ ) metric is hard to improve monotonically—it even starts to drop after prolonged training—while  $Pass@1$  remains comparatively stable and rarely collapses, we seek to boost  $Pass@K$  without degrading  $Pass@1$ . Figure 7 plots  $Pass@128$  against  $Pass@1$  under a variety of experimental settings. It shows that, at any fixed  $Pass@1$  level, our DARS

method delivers a consistently higher  $Pass@128$  than the other settings.

It is worth noting that, unlike the naive approach of simply increasing the rollout size to 32, our DARS achieves significantly higher training efficiency by allocating more rollouts to the hard problems. As shown in Table 2, our DARS methods need far fewer rollouts than the Depth-Naive method while achieve better performance.

**Depth-Breadth are Complementary in RLVR.** We show that Depth and Breadth are two complementary dimensions in RLVR. As shown in Figure 8, we present the  $Pass@1$ - $Pass@K$  training-dynamics curves for the Breadth, Depth, and the two-dimensional synergy approach DARS-Breadth. The farther the  $Pass@1$ - $Pass@K$  curve deviates outward, the more powerful the method. Our DARS-Breadth curves lie on the outermost envelope: it not only achieves the best  $Pass@1$ , but also simultaneously lifts  $Pass@K$ . This demonstrates the complementary roles of Depth and Breadth.

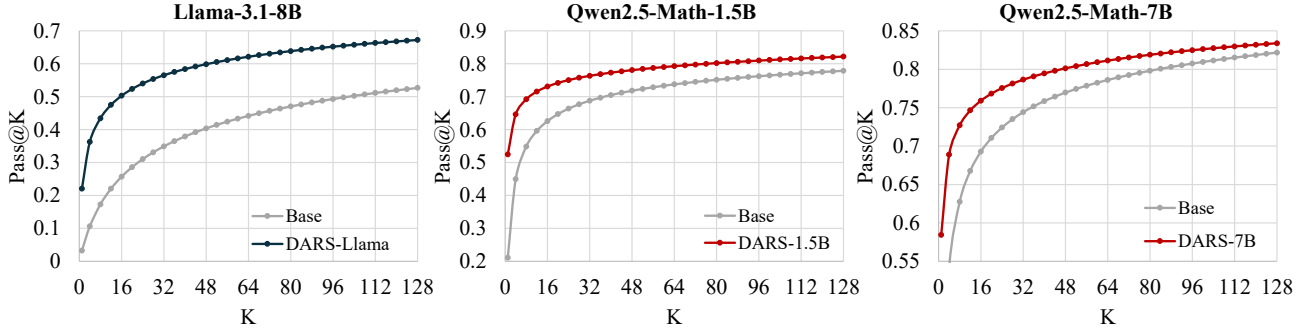


Figure 9. Complete  $Pass@K$  accuracy curve of base models and our DARS models.

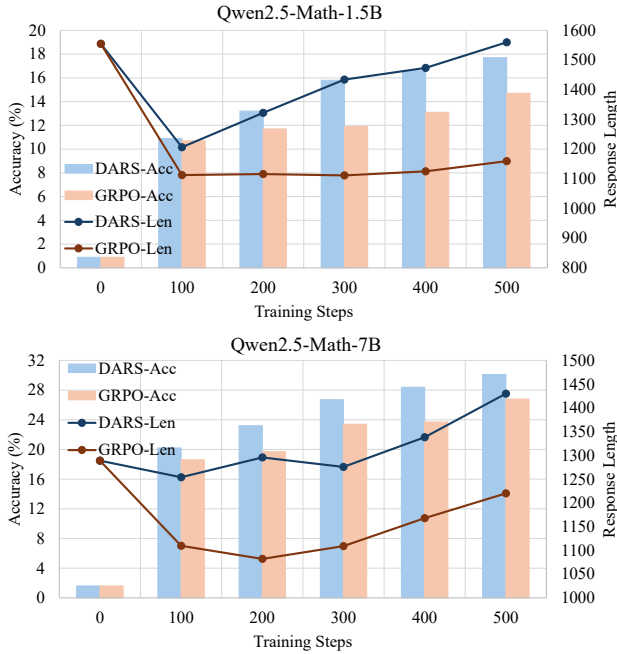


Figure 10. Comparison of our DARS-HW and GRPO-Baseline on AIME 2024. We show the average response length and accuracy for Qwen2.5-Math-1.5B and Qwen2.5-Math-7B. After training with DARS, the models can achieve higher accuracy by utilizing longer thinking process.

**Ablation Study on Base Model.** We further illustrate the effectiveness of DARS on Llama-3.1-8B. The results are shown in Table 3. Our DARS-ET-Breadth achieves both the highest  $Pass@1$  and  $Pass@128$  performance, which further illustrates the effectiveness of our method. DARS also consistently improves the performance of openPangu (Chen et al., 2025), as shown in Appendix E.

**DARS Elicits Longer Thought.** We tracked the response length dynamics during the training of DARS and GRPO. As shown in Figure 10, on the challenging AIME 2024 benchmark, DARS consistently produces longer reasoning traces than the baseline and has higher accuracy. These results reveal that our DARS stimulates the model to perform deeper thinking to solve hard problems.

**Complete  $Pass@K$  Accuracy Curve.** We show the complete  $Pass@K$  curve for Llama-3.1-8B, Qwen2.5-Math-1.5B, and Qwen2.5-Math-7B in Figure 9. The 3 chosen models of DARS are: DARS-Llama-ET-Breadth, DARS-1.5B-HW-Breadth, and DARS-7B-HW-Breadth. DARS models demonstrate a breakthrough in the reasoning boundaries of the base model, especially on the Llama-3.1-8B model, where the improvement in  $Pass@k$  is particularly significant.

## 5. Related Works

Reinforcement Learning (RL) is now standard in post-training LLMs. After early reward-model pipelines (Ouyang et al., 2022a), Direct Preference Optimization (Rafailov et al., 2023) streamlined training by exploiting pairwise preferences. RL with verifiable rewards (RLVR) has since pushed reasoning benchmarks in math and code, culminating in OpenAI’s o1 (Jaech et al., 2024) and the zero-RL breakthrough of DeepSeek-R1 (Guo et al., 2025). Follow-up Large Reasoning Models—Kimi 1.5 (Team et al., 2025), Gemini-Think (DeepMind, 2024), QwQ (Qwen, 2024), and studies like (Zeng et al., 2025; Luo et al., 2025) further validate RLVR. The leading algorithm, GRPO (Shao et al., 2024), extends PPO (Schulman et al., 2017) with group-relative advantages, inspiring DAPO (Yu et al., 2025), VAPO (Yue et al., 2025b), and Dr. GRPO (Liu et al., 2025b). Yet GRPO and its variants systematically undervalue hard problems, hurting  $Pass@K$ . More related works are shown in Appendix A.

## 6. Conclusion

In this work, we reveal that GRPO-based RLVR methods under-weight hard problems due to cumulative-advantage bias, capping  $Pass@K$ . Our DARS sampler cheaply re-allocates rollouts to these hard instances, while large-breadth training with full-batch updates raises  $Pass@1$ . The unified DARS-Breadth framework jointly lifts  $Pass@1$  and  $Pass@K$ , proving depth and breadth are synergistic levers in RLVR.

## Impact Statement

This paper presents work whose goal is to advance the field of Machine Learning. There are many potential societal consequences of our work, none which we feel must be specifically highlighted here

## References

- Achiam, J., Adler, S., Agarwal, S., Ahmad, L., Akkaya, I., Aleman, F. L., Almeida, D., Altenschmidt, J., Altman, S., Anadkat, S., et al. Gpt-4 technical report. *arXiv preprint arXiv:2303.08774*, 2023.
- Chen, H., Wang, Y., Han, K., Li, D., Li, L., Bi, Z., Li, J., Wang, H., Mi, F., Zhu, M., et al. Pangu embedded: An efficient dual-system llm reasoner with metacognition. *arXiv preprint arXiv:2505.22375*, 2025.
- Chen, M., Tworek, J., Jun, H., Yuan, Q., de Oliveira Pinto, H. P., Kaplan, J., Edwards, H., Burda, Y., Joseph, N., Brockman, G., Ray, A., Puri, R., Krueger, G., Petrov, M., Khlaaf, H., Sastry, G., Mishkin, P., Chan, B., Gray, S., Ryder, N., Pavlov, M., Power, A., Kaiser, L., Bavarian, M., Winter, C., Tillet, P., Such, F. P., Cummings, D., Plappert, M., Chantzis, F., Barnes, E., Herbert-Voss, A., Guss, W. H., Nichol, A., Paino, A., Tezak, N., Tang, J., Babuschkin, I., Balaji, S., Jain, S., Saunders, W., Hesse, C., Carr, A. N., Leike, J., Achiam, J., Misra, V., Morikawa, E., Radford, A., Knight, M., Brundage, M., Murati, M., Mayer, K., Welinder, P., McGrew, B., Amodei, D., McCandlish, S., Sutskever, I., and Zaremba, W. Evaluating large language models trained on code. 2021.
- Dang, X., Baek, C., Kolter, J. Z., and Raghunathan, A. Assessing diversity collapse in reasoning. In *Scaling Self-Improving Foundation Models without Human Supervision*, 2025.
- DeepMind, G. Gemini 2.0 flash thinking, 2024. URL <https://deepmind.google/technologies/gemini/flash-thinking/>.
- Fu, Y., Chen, T., Chai, J., Wang, X., Tu, S., Yin, G., Lin, W., Zhang, Q., Zhu, Y., and Zhao, D. Srft: A single-stage method with supervised and reinforcement fine-tuning for reasoning. *arXiv preprint arXiv:2506.19767*, 2025.
- Gandhi, K., Chakravarthy, A., Singh, A., Lile, N., and Goodman, N. D. Cognitive behaviors that enable self-improving reasoners, or, four habits of highly effective stars. *arXiv preprint arXiv:2503.01307*, 2025.
- Grattafiori, A., Dubey, A., Jauhri, A., Pandey, A., Kadian, A., Al-Dahle, A., Letman, A., Mathur, A., Schelten, A., Vaughan, A., et al. The llama 3 herd of models. *arXiv preprint arXiv:2407.21783*, 2024.
- Guo, D., Yang, D., Zhang, H., Song, J., Zhang, R., Xu, R., Zhu, Q., Ma, S., Wang, P., Bi, X., et al. Deepseek-r1: Incentivizing reasoning capability in llms via reinforcement learning. *arXiv preprint arXiv:2501.12948*, 2025.
- He, C., Luo, R., Bai, Y., Hu, S., Thai, Z., Shen, J., Hu, J., Han, X., Huang, Y., Zhang, Y., Liu, J., Qi, L., Liu, Z., and Sun, M. OlympiadBench: A challenging benchmark for promoting AGI with olympiad-level bilingual multimodal scientific problems. In Ku, L.-W., Martins, A., and Sriku-mar, V. (eds.), *Proceedings of the 62nd Annual Meeting of the Association for Computational Linguistics (Volume 1: Long Papers)*, pp. 3828–3850, Bangkok, Thailand, August 2024. Association for Computational Linguistics. doi: 10.18653/v1/2024.acl-long.211. URL <https://aclanthology.org/2024.acl-long.211/>.
- Hugging Face. Open r1: A fully open reproduction of deepseek-r1, January 2025. URL <https://github.com/huggingface/open-r1>.
- Jaech, A., Kalai, A., Lerer, A., Richardson, A., El-Kishky, A., Low, A., Helyar, A., Madry, A., Beutel, A., Carney, A., et al. Openai o1 system card. *arXiv preprint arXiv:2412.16720*, 2024.
- Karan, A. and Du, Y. Reasoning with sampling: Your base model is smarter than you think, 2025. URL <https://arxiv.org/abs/2510.14901>.
- Lewkowycz, A., Andreassen, A., Dohan, D., Dyer, E., Michalewski, H., Ramasesh, V., Slone, A., Anil, C., Schlag, I., Gutman-Solo, T., Wu, Y., Neysshabur, B., Gur-Ari, G., and Misra, V. Solving quantitative reasoning problems with language models. In Koyejo, S., Mohamed, S., Agarwal, A., Belgrave, D., Cho, K., and Oh, A. (eds.), *Advances in Neural Information Processing Systems*, volume 35, pp. 3843–3857. Curran Associates, Inc., 2022.
- Liang, X., Li, Z., Gong, Y., Shen, Y., Wu, Y. N., Guo, Z., and Chen, W. Beyond pass@ 1: Self-play with variational problem synthesis sustains rlvr. *arXiv preprint arXiv:2508.14029*, 2025.
- Lightman, H., Kosaraju, V., Burda, Y., Edwards, H., Baker, B., Lee, T., Leike, J., Schulman, J., Sutskever, I., and Cobbe, K. Let’s verify step by step. *arXiv preprint arXiv:2305.20050*, 2023.
- Liu, Z., Chen, C., Li, W., Pang, T., Du, C., and Lin, M. There may not be aha moment in r1-zero-like training—a pilot study, 2025a.
- Liu, Z., Chen, C., Li, W., Qi, P., Pang, T., Du, C., Lee, W. S., and Lin, M. Understanding r1-zero-like training: A critical perspective. *arXiv preprint arXiv:2503.20783*, 2025b.

- Luo, M., Tan, S., Wong, J., Shi, X., Tang, W. Y., Roongta, M., Cai, C., Luo, J., Li, L. E., Popa, R. A., and Stoica, I. Deepscaler: Surpassing o1-preview with a 1.5b model by scaling rl, 2025. Notion Blog.
- Ni, K., Tan, Z., Liu, Z., Li, P., and Chen, T. Can grpo help llms transcend their pretraining origin?, 2025. URL <https://arxiv.org/abs/2510.15990>.
- Ouyang, L., Wu, J., Jiang, X., Almeida, D., Wainwright, C., Mishkin, P., Zhang, C., Agarwal, S., Slama, K., Ray, A., et al. Training language models to follow instructions with human feedback. *NeurIPS*, 2022a.
- Ouyang, L., Wu, J., Jiang, X., Almeida, D., Wainwright, C. L., Mishkin, P., Zhang, C., Agarwal, S., Slama, K., Ray, A., Schulman, J., Hilton, J., Kelton, F., Miller, L., Simens, M., Askell, A., Welinder, P., Christiano, P., Leike, J., and Lowe, R. Training language models to follow instructions with human feedback, 2022b. URL <https://arxiv.org/abs/2203.02155>.
- Qin, T., Park, C. F., Kwun, M., Walsman, A., Malach, E., Anand, N., Tanaka, H., and Alvarez-Melis, D. Decomposing elements of problem solving: What "math" does rl teach?, 2025. URL <https://arxiv.org/abs/2505.22756>.
- Qwen. Qwq-32b: Embracing the power of reinforcement learning, 2024. URL <https://qwenlm.github.io/blog/qwq-32b/>.
- Rafailov, R., Sharma, A., Mitchell, E., Manning, C. D., Ermon, S., and Finn, C. Direct preference optimization: Your language model is secretly a reward model. *NeurIPS*, 2023.
- Schulman, J., Wolski, F., Dhariwal, P., Radford, A., and Klimov, O. Proximal policy optimization algorithms. *arXiv preprint arXiv:1707.06347*, 2017.
- Shah, D. J., Rushton, P., Singla, S., Parmar, M., Smith, K., Vanjani, Y., Vaswani, A., Chaluvaraju, A., Hojel, A., Ma, A., et al. Rethinking reflection in pre-training. *arXiv preprint arXiv:2504.04022*, 2025.
- Shao, Z., Wang, P., Zhu, Q., Xu, R., Song, J., Bi, X., Zhang, H., Zhang, M., Li, Y. K., Wu, Y., and Guo, D. Deepseekmath: Pushing the limits of mathematical reasoning in open language models, 2024. URL <https://arxiv.org/abs/2402.03300>.
- Sheng, G., Zhang, C., Ye, Z., Wu, X., Zhang, W., Zhang, R., Peng, Y., Lin, H., and Wu, C. Hybridflow: A flexible and efficient rlhf framework. *arXiv preprint arXiv:2409.19256*, 2024.
- Tajwar, F., Zeng, G., Zhou, Y., Song, Y., Arora, D., Jiang, Y., Schneider, J., Salakhutdinov, R., Feng, H., and Zanette, A. Maximum likelihood reinforcement learning, 2026. URL <https://arxiv.org/abs/2602.02710>.
- Team, K., Du, A., Gao, B., Xing, B., Jiang, C., Chen, C., Li, C., Xiao, C., Du, C., Liao, C., et al. Kimi k1. 5: Scaling reinforcement learning with llms. *arXiv preprint arXiv:2501.12599*, 2025.
- Wang, Z., Zhou, F., Li, X., and Liu, P. Octothinker: Mid-training incentivizes reinforcement learning scaling. *arXiv preprint arXiv:2506.20512*, 2025.
- Yan, J., Li, Y., Hu, Z., Wang, Z., Cui, G., Qu, X., Cheng, Y., and Zhang, Y. Learning to reason under off-policy guidance, 2025. URL <https://arxiv.org/abs/2504.14945>.
- Yang, A., Zhang, B., Hui, B., Gao, B., Yu, B., Li, C., Liu, D., Tu, J., Zhou, J., Lin, J., Lu, K., Xue, M., Lin, R., Liu, T., Ren, X., and Zhang, Z. Qwen2.5-math technical report: Toward mathematical expert model via self-improvement, 2024. URL <https://arxiv.org/abs/2409.12122>.
- Yu, Q., Zhang, Z., Zhu, R., Yuan, Y., Zuo, X., Yue, Y., Dai, W., Fan, T., Liu, G., Liu, L., Liu, X., Lin, H., Lin, Z., Ma, B., Sheng, G., Tong, Y., Zhang, C., Zhang, M., Zhang, W., Zhu, H., Zhu, J., Chen, J., Chen, J., Wang, C., Yu, H., Song, Y., Wei, X., Zhou, H., Liu, J., Ma, W.-Y., Zhang, Y.-Q., Yan, L., Qiao, M., Wu, Y., and Wang, M. Dapo: An open-source llm reinforcement learning system at scale, 2025. URL <https://arxiv.org/abs/2503.14476>.
- Yue, Y., Chen, Z., Lu, R., Zhao, A., Wang, Z., Song, S., and Huang, G. Does reinforcement learning really incentivize reasoning capacity in llms beyond the base model? *arXiv preprint arXiv:2504.13837*, 2025a.
- Yue, Y., Yuan, Y., Yu, Q., Zuo, X., Zhu, R., Xu, W., Chen, J., Wang, C., Fan, T., Du, Z., Wei, X., Yu, X., Liu, G., Liu, J., Liu, L., Lin, H., Lin, Z., Ma, B., Zhang, C., Zhang, M., Zhang, W., Zhu, H., Zhang, R., Liu, X., Wang, M., Wu, Y., and Yan, L. Vapo: Efficient and reliable reinforcement learning for advanced reasoning tasks, 2025b. URL <https://arxiv.org/abs/2504.05118>.
- Zeng, W., Huang, Y., Liu, Q., Liu, W., He, K., Ma, Z., and He, J. Simplerl-zoo: Investigating and taming zero reinforcement learning for open base models in the wild. *arXiv preprint arXiv:2503.18892*, 2025.
- Zhao, R., Metereez, A., Kakade, S., Pehlevan, C., Jelassi, S., and Malach, E. Echo chamber: RL post-training amplifies behaviors learned in pretraining. *arXiv preprint arXiv:2504.07912*, 2025.

## Appendix

### A. More Related Works

With the rapid advancement of RLVR and the proliferation of open-source LRMs, many studies have begun to analyze the RLVR pipeline and these open LRMs. Several studies (Liu et al., 2025a; Zhao et al., 2025; Shah et al., 2025) indicates that the self-reflect and self-critique behaviors observed after RLVR originates from the base model rather than the RL process. (Dang et al., 2025) find that although the RLVR process benefits  $Pass@1$ ,  $Pass@K$  may decline as training progresses. Subsequently, (Yue et al., 2025a) through extensive experimental analysis, discovered that RLVR’s performance is significantly constrained by the base model; once training converges, it struggles to surpass the capability boundary of the base model. These studies have sparked widespread concern about the capability ceiling of RLVR, and consequently, the  $Pass@K$  metric has become a focal point for diagnosing and potentially transcending the intrinsic limits imposed by the base model (Liang et al., 2025). This paper analyzes and refines the RLVR pipeline from the dual perspectives of  $Pass@1$  and  $Pass@K$ .

### B. Mathematical Derivations for DARS and GRPO Training Dynamics

#### B.1. Derivation of Additional Rollouts $\Delta n_j$

The cumulative advantage for a group with accuracy  $\hat{a}_j$  and total rollout size  $N_j = N^{pre} + \Delta n_j$  is given by:

$$\mathcal{A}_{\text{group}}(\hat{a}_j, N_j) = N_j \cdot \mathcal{S}(\hat{a}_j),$$

where  $\mathcal{S}(\hat{a}_j) = 2\hat{a}_j(1 - \hat{a}_j)$ .

After the first-stage rollout of size  $N^{pre}$ , the initial cumulative advantage is:

$$\mathcal{A}_{\text{group}}^{N^{pre}}(\hat{a}_j) = N^{pre} \cdot \mathcal{S}(\hat{a}_j).$$

Our goal is to determine the number of additional trajectories  $\Delta n_j$  needed so that the final cumulative advantage  $\mathcal{A}_{\text{group}}(\hat{a}_j, N_j)$  meets a target value  $\mathcal{A}_{\text{group}}^{\text{target}}(\hat{a}_j)$ .

#### Equal-Treatment (ET) Schedule:

The target cumulative advantage is set to be constant for all questions with  $\hat{a}_j < 0.5$ :

$$\mathcal{A}_{\text{group}}^{\text{ET}}(\hat{a}_j) = \mathcal{A}_{\text{group}}^{N^{pre}}(0.5) = N^{pre} \cdot \mathcal{S}(0.5).$$

We solve for  $\Delta n_j^{\text{ET}}$ :

$$\begin{aligned} \mathcal{A}_{\text{group}}(\hat{a}_j, N_j) &= \mathcal{A}_{\text{group}}^{\text{ET}}(\hat{a}_j) \\ (N^{pre} + \Delta n_j^{\text{ET}}) \cdot \mathcal{S}(\hat{a}_j) &= N^{pre} \cdot \mathcal{S}(0.5) \\ \Delta n_j^{\text{ET}} \cdot \mathcal{S}(\hat{a}_j) &= N^{pre} \cdot \mathcal{S}(0.5) - N^{pre} \cdot \mathcal{S}(\hat{a}_j) \\ \Delta n_j^{\text{ET}} &= \frac{N^{pre} \cdot \mathcal{S}(0.5) - N^{pre} \cdot \mathcal{S}(\hat{a}_j)}{\mathcal{S}(\hat{a}_j)}. \\ \Delta n_j^{\text{ET}} &= \frac{\mathcal{A}_{\text{group}}^{N^{pre}}(0.5) - \mathcal{A}_{\text{group}}^{N^{pre}}(\hat{a}_j)}{\mathcal{S}(\hat{a}_j)}. \end{aligned}$$

The rollout size must be an integer, and we cap the total rollout sampling upper limit at  $N^{\max}$ , so

$$\Delta n_j^{\text{ET}} = \min\left(\left\lceil \frac{\mathcal{A}_{\text{group}}^{N^{pre}}(0.5) - \mathcal{A}_{\text{group}}^{N^{pre}}(\hat{a}_j)}{\mathcal{S}(\hat{a}_j)} \right\rceil, N^{\max} - N^{pre}\right).$$

#### Hardness-Weighted (HW) Schedule:

The target cumulative advantage increases with difficulty:

$$\mathcal{A}_{\text{group}}^{\text{HW}}(\hat{a}_j) = 2(1 - \hat{a}_j) \cdot \mathcal{A}_{\text{group}}^N(0.5) = 2x_j \cdot N^{\text{pre}} \cdot \mathcal{S}(0.5).$$

We solve for  $\Delta n_j^{\text{HW}}$ :

$$\begin{aligned} \mathcal{A}_{\text{group}}(\hat{a}_j, N_j) &= \mathcal{A}_{\text{group}}^{\text{HW}}(\hat{a}_j) \\ (N^{\text{pre}} + \Delta n_j^{\text{HW}}) \cdot \mathcal{S}(\hat{a}_j) &= 2x_j \cdot N^{\text{pre}} \cdot \mathcal{S}(0.5) \\ \Delta n_j^{\text{HW}} \cdot \mathcal{S}(\hat{a}_j) &= 2x_j \cdot N^{\text{pre}} \cdot \mathcal{S}(0.5) - N^{\text{pre}} \cdot \mathcal{S}(\hat{a}_j) \\ \Delta n_j^{\text{HW}} &= \frac{2x_j \cdot N^{\text{pre}} \cdot \mathcal{S}(0.5) - N^{\text{pre}} \cdot \mathcal{S}(\hat{a}_j)}{\mathcal{S}(\hat{a}_j)}. \end{aligned}$$

Again, using the baseline advantage notation  $\mathcal{A}_{\text{group}}^{N^{\text{pre}}}(\hat{a}_j) = N^{\text{pre}} \cdot \mathcal{S}(\hat{a}_j)$ , we obtain:

$$\Delta n_j^{\text{HW}} = \min\left(\left\lceil \frac{2x_j \cdot \mathcal{A}_{\text{group}}^{N^{\text{pre}}}(0.5) - \mathcal{A}_{\text{group}}^{N^{\text{pre}}}(\hat{a}_j)}{\mathcal{S}(\hat{a}_j)} \right\rceil, N^{\text{max}} - N^{\text{pre}}\right).$$

Both derivations include a ceiling function and are capped at  $N^{\text{max}}$  to control computational cost, as shown in Equations 6 and 8 in the paper.

## B.2. Connection of Expected Squared Gradient Norm and Group Cumulative Advantage

In this subsection, we will prove that: in the setting of group-relative advantages, the *expected squared gradient norm* allocated to a problem is proportional to the group cumulative advantage  $\mathcal{A}_{\text{group}}$ .

### Proposition B.1

In a Reinforcement Learning with Verifiable Reward (RLVR) setting utilizing group-relative advantages, the expected squared gradient norm of a problem group is directly proportional to its Group Cumulative Advantage  $\mathcal{A}_{\text{group}}$ .

*Proof.* By definition, for a specific problem  $q$ , the group gradient  $\mathbf{g}_{\text{group}}$  before taking the dataset expectation is formulated at the trajectory level as:

$$\mathbf{g}_{\text{group}} = \frac{1}{G} \sum_{i=1}^G \hat{A}_i \nabla_{\theta} \log \pi_{\theta}(o_i | q), \quad (11)$$

where  $o_i$  denotes the  $i$ -th sampled trajectory. Let  $\mathbf{g}_i \triangleq \nabla_{\theta} \log \pi_{\theta}(o_i | q)$  denote the score function of the trajectory. To evaluate the optimization step size, we compute the expected squared  $L_2$  norm of the group gradient:

$$\mathbb{E} [\|\mathbf{g}_{\text{group}}\|^2] = \frac{1}{G^2} \mathbb{E} \left[ \sum_{i=1}^G \hat{A}_i^2 \|\mathbf{g}_i\|^2 + \sum_{i \neq j} \hat{A}_i \hat{A}_j \langle \mathbf{g}_i, \mathbf{g}_j \rangle \right]. \quad (12)$$

While the cross terms  $\mathbb{E}[\hat{A}_i \hat{A}_j \langle \mathbf{g}_i, \mathbf{g}_j \rangle]$  do not strictly vanish (since the advantages  $\hat{A}_i$  and  $\hat{A}_j$  are coupled through the group mean reward and correlated with the score functions), they are heavily dominated by the diagonal terms in the context of Large Language Models (LLMs).

In the enormously high-dimensional parameter space typical of LLMs, the policy gradient estimator exhibits notoriously high variance. The individual trajectory gradients  $\mathbf{g}_i$  are highly stochastic and point in nearly orthogonal directions. Consequently, the inner product of different trajectory gradients  $\langle \mathbf{g}_i, \mathbf{g}_j \rangle$  is exceedingly small compared to the squared norm of a single trajectory gradient  $\|\mathbf{g}_i\|^2$ . Mathematically, the diagonal sum represents the uncentered variance (update energy) of the samples, while the cross-terms correspond to the squared norm of the expected gradient  $\|\mathbb{E}[\mathbf{g}_{\text{group}}]\|^2$ . In RL for LLMs, the

gradient noise variance inherently dwarfs the true gradient magnitude (i.e.,  $\text{Tr}(\text{Var}(\hat{A}_i \mathbf{g}_i)) \gg \|\mathbb{E}[\hat{A}_i \mathbf{g}_i]\|^2$ ). Therefore, we can safely approximate the expected squared group gradient by its dominant diagonal components:

$$\mathbb{E} [\|\mathbf{g}_{\text{group}}\|^2] \approx \frac{1}{G^2} \mathbb{E} \left[ \sum_{i=1}^G \hat{A}_i^2 \|\mathbf{g}_i\|^2 \right]. \quad (13)$$

Let  $V^2 = \mathbb{E}[\|\mathbf{g}_i\|^2]$  denote the expected squared norm of the trajectory gradient (which corresponds to the trace of the Fisher Information Matrix). Under the standard simplifying assumption that the gradient magnitude is approximately independent of the specific binary correctness  $r_i$ , we can decouple the expectations. This elegantly isolates the advantage term, simplifying the expected squared group gradient to:

$$\mathbb{E} [\|\mathbf{g}_{\text{group}}\|^2] \approx \frac{V^2}{G^2} \mathbb{E} \left[ \sum_{i=1}^G \hat{A}_i^2 \right]. \quad (14)$$

We now evaluate the advantage term  $\sum_{i=1}^G \hat{A}_i^2$ . In RLVR, verifiable rewards are binary, i.e.,  $r_i \in \{0, 1\}$ . Without standard-deviation normalization, the advantage is computed as  $\hat{A}_i = r_i - u$ , where  $u$  is the expected group mean reward. The sum of squared advantages expands algebraically as:

$$\begin{aligned} \mathbb{E} \left[ \sum_{i=1}^G \hat{A}_i^2 \right] &= \sum_{i:r_i=1} (1-u)^2 + \sum_{i:r_i=0} (-u)^2 \\ &= c(1-u)^2 + (G-c)u^2 \\ &= Gu(1-u)^2 + G(1-u)u^2 \\ &= Gu(1-u)[(1-u) + u] = Gu(1-u). \end{aligned} \quad (15)$$

Simultaneously, the Group Cumulative Advantage  $\mathcal{A}_{\text{group}}$  is defined as the sum of absolute advantages:

$$\begin{aligned} \mathbb{E} [\mathcal{A}_{\text{group}}] &= \sum_{i=1}^G |\hat{A}_i| = \sum_{i:r_i=1} |1-u| + \sum_{i:r_i=0} |-u| \\ &= c(1-u) + (G-c)u \\ &= Gu(1-u) + G(1-u)u = 2Gu(1-u). \end{aligned} \quad (16)$$

Comparing Equation 15 and Equation 16 reveals a strict algebraic identity unique to the binary group-relative advantage formulation:

$$\mathbb{E} \left[ \sum_{i=1}^G \hat{A}_i^2 \right] \equiv \frac{1}{2} \mathbb{E} [\mathcal{A}_{\text{group}}]. \quad (17)$$

Substituting Equation 17 into Equation 14, we obtain the final exact proportionality:

$$\mathbb{E} [\|\mathbf{g}_{\text{group}}\|^2] \approx \left( \frac{V^2}{2G^2} \right) \mathbb{E} [\mathcal{A}_{\text{group}}] = 2Gu(1-u). \quad (18)$$

This demonstrates that the expected optimization step size (squared gradient norm) is strictly proportional to the Group Cumulative Advantage.  $\square$

**Theoretical Implications.** Proposition B.2 fundamentally justifies our algorithmic design. By demonstrating that the expected variance (i.e., update energy) of the parameter gradient is mathematically locked to  $\mathcal{A}_{\text{group}}$ , we confirm that  $\mathcal{A}_{\text{group}}$  acts as a rigorous surrogate for the gradient signal strength allocated to each problem. This mathematically verifies that existing GRPO variants intrinsically under-update hard problems (where  $\mathcal{A}_{\text{group}}$  is distortedly low), directly motivating the necessity of our Difficulty Adaptive Rollout Sampling (DARS) methodology to re-balance update magnitudes.

## C. Theoretical Connection Between DARS and Maximum Likelihood Reinforcement Learning

Recent work on Maximum Likelihood Reinforcement Learning (MaxRL) (Tajwar et al., 2026) demonstrates that standard expected-reward objectives systematically under-weight high-difficulty instances. To counteract this, MaxRL introduces a modified advantage function to approximate the Maximum Likelihood (ML) objective.

In this section, we provide a formal theoretical analysis demonstrating that **our Difficulty-Adaptive Rollout Sampling (DARS) with the Hardness-Weighted (HW) schedule optimizes an expected objective identical to MaxRL**. Crucially, we prove that while MaxRL relies on algebraic advantage scaling, which inherently exacerbates gradient variance. While DARS achieves the same objective through physical compute reallocation. We establish that DARS serves as a strict variance-reduced estimator of the ML-equivalent objective, offering superior optimization stability.

### C.1. Objective Equivalence via Cumulative Advantage

We first analyze the weighting behavior of both algorithms utilizing our proposed Group Cumulative Advantage ( $\mathcal{A}_{group}$ ) framework. Let  $N$  denote the number of rollouts for a given prompt  $q$ , and let  $u \in (0, 1)$  denote the mean reward (i.e., empirical accuracy or pass rate), where the binary reward is  $r_i \in \{0, 1\}$ .

#### Proposition C.1 (Equivalence of Difficulty Weighting Profile)

Both MaxRL and DARS-HW impose a problem-level optimization weight that is strictly proportional to  $(1 - u)$ . Consequently, both algorithms share an identical inductive bias: linearly up-weighting the optimization focus on problems as their difficulty increases ( $u \rightarrow 0$ ).

*Proof.* For MaxRL, the advantage is scaled as  $\hat{A}_i^{MaxRL} = \frac{r_i - u}{u}$ . For a group of  $N$  rollouts, the expected number of successful trajectories ( $r_i = 1$ ) is  $Nu$ , and the expected number of failed trajectories ( $r_i = 0$ ) is  $N(1 - u)$ . The cumulative advantage is thus computed as:

$$\begin{aligned} \mathcal{A}_{group}^{MaxRL}(u) &= \mathbb{E} \left[ \sum_{i=1}^N \left| \hat{A}_i^{MaxRL} \right| \right] \\ &= Nu \cdot \left| \frac{1 - u}{u} \right| + N(1 - u) \cdot \left| \frac{0 - u}{u} \right| \\ &= N(1 - u) + N(1 - u) = 2N(1 - u) \end{aligned}$$

For DARS-HW, we employ the unscaled advantage  $\hat{A}_i = r_i - u$ . Based on our proposed schedule (Equation 7), the target cumulative advantage is explicitly constrained to:

$$\mathcal{A}_{group}^{HW}(u) = 2(1 - u)\mathcal{A}_{group}^{N_{pre}}(0.5) = C \cdot (1 - u)$$

where  $C = 2\mathcal{A}_{group}^{N_{pre}}(0.5)$  is a constant independent of the prompt difficulty  $u$ . Since  $\mathcal{A}_{group}^{MaxRL}(u) \propto (1 - u)$  and  $\mathcal{A}_{group}^{HW}(u) \propto (1 - u)$ , the weighting profiles are equivalent.  $\square$

### C.2. Equivalence of Expected Gradients

To formalize the alignment in optimization trajectories, we compare the total expected gradient contribution of a single prompt  $q$  under both methods. Let  $\nabla J_i(u) = (r_i - u)\nabla_{\theta} \log \pi_{\theta}(o_i|q)$  denote the standard baseline-subtracted policy gradient for a single rollout.

#### Proposition C.2 (Equivalence of Expected Gradient Updates)

Let  $K$  be a positive scalar. The expected gradient updates of MaxRL and DARS-HW are proportional:  $\mathbb{E}[\nabla J_q^{MaxRL}] \propto \mathbb{E}[\nabla J_q^{DARS-HW}] \propto \frac{1}{u}\mathbb{E}[\nabla J_i(u)]$ . Both methods approximate the Maximum Likelihood gradient by universally scaling the standard policy gradient by a factor of  $1/u$ .

*Proof.* For MaxRL, using a fixed rollout size  $N$ , the total expected gradient is scaled algebraically:

$$\mathbb{E}[\nabla J_q^{MaxRL}] = \mathbb{E}\left[\sum_{i=1}^N \frac{r_i - u}{u} \nabla_{\theta} \log \pi_{\theta}(o_i|q)\right] = \frac{N}{u} \cdot \mathbb{E}[\nabla J_i(u)]$$

For DARS-HW, we dynamically adjust the rollout size  $N_{DARS}(u)$  to match the target  $\mathcal{A}_{group}^{HW}(u) = C(1-u)$ . Recall the standard group cumulative advantage property  $\mathcal{A}_{group} = 2N_{DARS}u(1-u)$ . Equating the two yields  $2N_{DARS}(u)u(1-u) = C(1-u)$ , which simplifies to  $N_{DARS}(u) = \frac{C}{2u}$ . Thus, the expected gradient contribution is:

$$\mathbb{E}[\nabla J_q^{DARS-HW}] = \mathbb{E}\left[\sum_{i=1}^{N_{DARS}(u)} (r_i - u) \nabla_{\theta} \log \pi_{\theta}(o_i|q)\right] = \frac{C}{2u} \cdot \mathbb{E}[\nabla J_i(u)]$$

Up to the constants  $N$  and  $C/2$ , both expected gradients scale strictly by  $1/u$ .  $\square$

### C.3. Variance Analysis: DARS-HW versus MaxRL

While Proposition C.2 establishes that DARS-HW and MaxRL optimize the same expected objective, they diverge significantly in their construction of the Monte Carlo gradient estimator. Let  $\Sigma_g = \text{Var}(\nabla J_i(u))$  denote the trace of the covariance matrix of the unscaled token-level gradient for a single rollout. We make the standard assumption that conditioned on the prompt  $q$  and current policy  $\pi_{\theta}$ , individual rollouts are independent and identically distributed (i.i.d.).

Let  $u \rightarrow 0$  denote the regime of increasingly difficult reasoning tasks. For the MaxRL estimator, the variance relies on algebraic scalar multiplication over a fixed  $N$  samples. By the properties of variance for i.i.d. variables ( $\text{Var}(aX) = a^2\text{Var}(X)$ ):

$$\text{Var}(\hat{\nabla} J_q^{MaxRL}) = \text{Var}\left(\sum_{i=1}^N \frac{1}{u} \nabla J_i(u)\right) = \sum_{i=1}^N \frac{1}{u^2} \text{Var}(\nabla J_i(u)) = \frac{N}{u^2} \Sigma_g$$

Conversely, DARS-HW physically expands the sampling space, drawing  $N_{DARS}(u) = \frac{C}{2u}$  independent trajectories while maintaining the bounded unscaled advantage  $|r_i - u| \leq 1$ :

$$\text{Var}(\hat{\nabla} J_q^{DARS-HW}) = \text{Var}\left(\sum_{i=1}^{N_{DARS}(u)} \nabla J_i(u)\right) = \sum_{i=1}^{N_{DARS}(u)} \text{Var}(\nabla J_i(u)) = N_{DARS}(u) \Sigma_g = \frac{C}{2u} \Sigma_g$$

Taking the ratio of the two variances yields:

$$\frac{\text{Var}(\hat{\nabla} J_q^{MaxRL})}{\text{Var}(\hat{\nabla} J_q^{DARS-HW})} = \frac{N/u^2}{C/(2u)} = \frac{2N}{C} \cdot \frac{1}{u} \propto \frac{1}{u}$$

Therefore, as  $u \rightarrow 0$ , the variance of MaxRL grows at a rate of  $\mathcal{O}(1/u^2)$ , while DARS-HW grows at a significantly slower rate of  $\mathcal{O}(1/u)$ .

### C.4. Theoretical Analysis Conclusions

- Unified Optimization Objective with Divergent Implementation Routes.** DARS-HW and MaxRL are two distinct implementation routes toward the same Maximum Likelihood reinforcement learning objective. MaxRL achieves the target optimization weight by *algebraically modifying the advantage function* ( $\hat{A}_i^{MaxRL} = \frac{r_i - u}{u}$ ), scaling the gradient signal of each rollout by  $1/u$ . In contrast, DARS-HW retains the original unscaled advantage function ( $\hat{A}_i = r_i - u$ ) and instead achieves the identical expected gradient scaling by *adaptively increasing the number of rollouts* ( $N_{DARS}(u) \propto 1/u$ ) for difficult problems. These two approaches are mathematically equivalent in expectation but differ fundamentally in their implementation strategy.
- Variance Reduction of DARS.** Appendix C.3 fundamentally explains the superiority of DARS over pure advantage-scaling methods as MaxRL. For complex reasoning tasks where the initial pass rate is extremely low ( $u \ll 1$ ), MaxRL heavily amplifies the gradient of rare, potentially idiosyncratic correct trajectories. This leads to a high-variance

gradient regime, which may inducing optimization instability and premature convergence. By contrast, DARS-HW functions as a variance-reduced estimator. Instead of amplifying a small fixed set of rollouts algebraically, DARS-HW allocates explicit computational budget to difficult problems, thereby expanding the breadth of **actual** correct reasoning paths discovered. This mechanism preserves a high signal-to-noise ratio in the gradient and maintains robust token-level entropy, theoretically validating DARS-HW as a more stable and efficient paradigm for Maximum Likelihood RL optimization.

### D. Training and Evaluation Details

**Prompt for Solving Complex Reasoning Tasks**

Your task is to solve the given question step by step. You should conduct a systematic, thorough reasoning process before providing the final answer. This involves analyzing, summarizing, exploring, reassessing, and refining your reasoning process through multiple iterations. Each reasoning step should include detailed analysis, brainstorming, verification, and refinement of ideas. You should include the final answer in `\boxed{}` for closed-form results like multiple choices or mathematical results.

**Parameters and Metrics.** Currently, our experiments are conducted with Qwen2.5-Math series language models (Yang et al., 2024). We set the temperature to 1.0 for both the training and evaluation procedures. In this paper, we mainly use two metrics, *Pass@1* and *Pass@K*. To acquire *Pass@K* results, we sample 128 candidate responses for each question during the evaluation process; the calculation of *Pass@1* is derived from *Avg@128*. Both the training and evaluation processes are scored using Math-Verify. The learning rate is 1e-6 for depth training methods, and 5e-6 for large breadth training. We do not use the reference model and KL loss. For fair comparison, we uniformly set the PPO mini step to 2 for all experiments. By default, the maximum prompt length is 1024, and the maximum response length is 3072 for the Qwen2.5-Math series model.

**Implementation Details.** Following LUFFY (Yan et al., 2025), we use the default subset and filter out generations that are longer than 8192 tokens and those that are verified wrong by Math-Verify<sup>1</sup>, resulting in 45k question-solution pairs. For training Llama-3.1-8B, we use the train split of MATH dataset. Our training framework is derived from Verl (Sheng et al., 2024) pipeline, which is a flexible, high-performance reinforcement-learning framework built for training large language-model agents. With native PyTorch support and efficient distributed training, Verl lets researchers quickly prototype and scale RL algorithms like PPO on GPUs. Following Dr. GRPO (Liu et al., 2025b), we remove the KL loss and the length normalization in GRPO. All of our experiments are conducted on H200 GPUs. At present, the LLM of our experiment is the Qwen2.5-Math series.

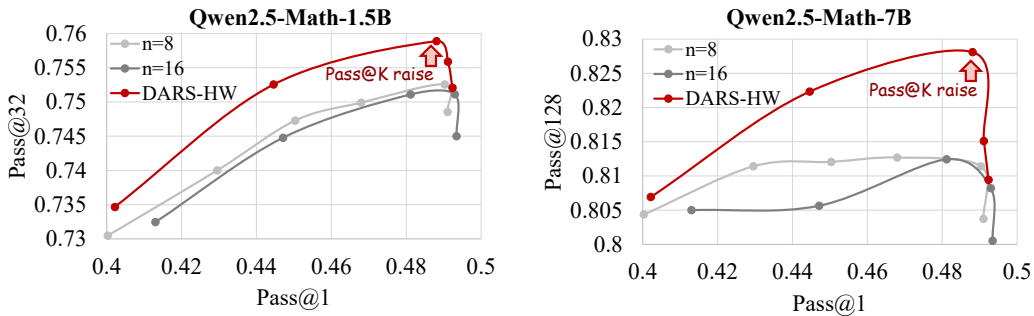


Figure 11. Comparison of our DARS on std-based advantage computation.

**Training Steps and Checkpoint Steps.** For non-breadth methods on Qwen2.5-Math-1.5B/7B, we set the checkpoint step as 100. For breadth methods on Qwen2.5-Math-1.5B/7B, we set the checkpoint step as 15. The specific training steps are determined according to the convergence of the model. The number of training steps for non-breadth training is set as 300 for Llama-3.1-8B, 600 for Qwen2.5-Math-1.5B, and 500 for Qwen2.5-Math-7B. The number of training steps for

<sup>1</sup><https://github.com/huggingface/Math-Verify>

breadth training is set as 70. For breadth training, we set the total training steps as 105 for Qwen2.5-Math-1.5B, and 75 for Qwen2.5-Math-7B.

## E. More Experimental Results

### E.1. Ablation Study on std-based Advantage Computation

As illustrated in Section 2, Dr. GRPO (Liu et al., 2025b) removes the standard-deviation term from the advantage computation to eliminate question-level difficulty bias, and demonstrates its superiority through extensive experiments. Consequently, the experiments reported in this study were conducted primarily through the Dr. GRPO methodology. To further illustrate the effectiveness of DARS on std-based advantage computation, we conduct the experiment with HW schedule on Qwen2.5-Math-1.5B model, as shown in Figure 11

### E.2. Depth and Breadth Synergy for Pass@1 and Pass@32

In Section 4.3, we show the training dynamics of  $Pass@128$ - $Pass@1$  for DARS and baseline methods. To further illustrate the effectiveness of DARS, we show the training dynamics of  $Pass@32$ - $Pass@1$  in Figure 13. Our DARS significantly improves the  $Pass@32$  performance compared to other methods.

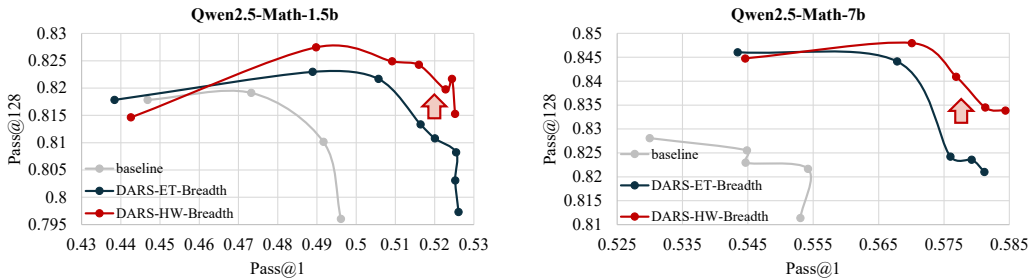


Figure 12. Comparison of ET and HW schedule in breadth training of Qwen2.5-Math series.

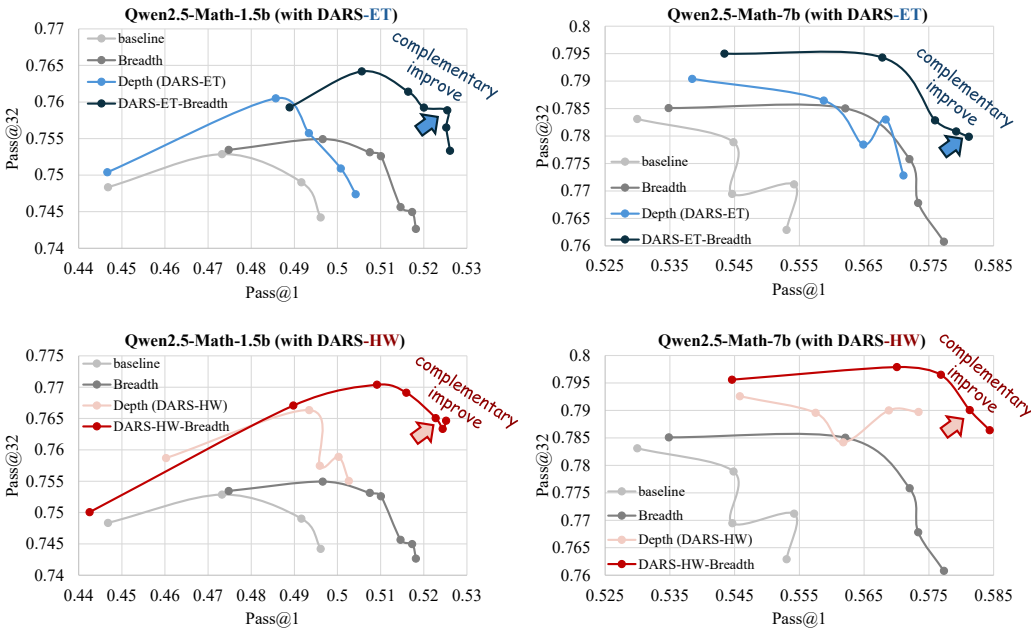


Figure 13. Complementary improve of Depth and Breadth Synergy for  $Pass@1$  and  $Pass@K$  ( $K=32$ ) performance.

### E.3. Comparison of ET/HW Schedule in Breadth Scaling

In addition, compared with the ET schedule, DARS-HW-Breadth significantly improves the model’s Pass@128 performance as shown in Figure 12. We consider this performance gain is due to the HW schedule placing greater emphasis on difficult samples.

	Qwen2.5-Math-1.5B					Qwen2.5-Math-7B				
	$t=0.6$	$t=0.8$	$t=1.0$	$t=1.2$	$t=1.4$	$t=0.6$	$t=0.8$	$t=1.0$	$t=1.2$	$t=1.4$
GRPO-Baseline	78.9	79.2	79.6	80	80	80.4	80.7	81.4	81.6	81.6
Depth-Naive	79.4	79.6	79.9	80.3	80.4	79.7	80	80.3	80.7	80.8
Breadth-Naive	78.9	78.9	79.2	79.6	79.9	77.7	78.1	79.2	79.4	79.6
DARS-HW-Breadth	<b>81.6</b>	<b>81.9</b>	<b>82.2</b>	<b>82.6</b>	<b>82.7</b>	<b>82.6</b>	<b>82.8</b>	<b>83.4</b>	<b>84.0</b>	<b>84.0</b>

Figure 14. Heat map of Pass@128 of Qwen2.5-Math series in different temperatures.

### E.4. Impact of Temperature

Some researches (Karan & Du, 2025; Qin et al., 2025; Ni et al., 2025) indicates that temperature matters in LLM reasoning. To further illustrate the performance improvement under different temperatures, we additionally add the above experiments. The results show that the improvement of our method is consistent over different temperatures. The results are shown in Figure 14.

### E.5. Consistent Improvement During RL Process

To further show that our method consistently improve model performance, we calculated the mean of Pass@128 and Pass@32 for the last 3 checkpoints of each method, as shown in Table 4.

Table 4. Average performance of Pass@1/32/128 for the last 3 checkpoints during training.

Model	Pass@1	Pass@32	Pass@128
<i>Qwen2.5-Math-1.5B as the Base Model</i>			
GRPO-Baseline	48.8	74.7	80.8
Depth-Naive	49.5	74.4	80.6
Breadth-Naive	51.4	74.4	79.8
DARS-HW	49.5	75.7	81.9
<b>DARS-HW-Breadth</b>	<b>52.4</b>	<b>76.4</b>	<b>82.1</b>
<i>Qwen2.5-Math-7B as the Base Model</i>			
GRPO-Baseline	55.1	76.9	81.8
Depth-Naive	56.4	76.7	80.9
Breadth-Naive	57.2	76.7	81.3
DARS-HW	56.8	78.8	83.4
<b>DARS-HW-Breadth</b>	<b>58.3</b>	<b>79.1</b>	<b>83.7</b>

### E.6. Performance of Other Model

We further evaluate our method on Qwen2.5-7B-Instruct. Following (Liang et al., 2025), we change the training data to Math12k. The results are shown in Table 5.

We further evaluate DARS with the openPangu-7B architecture on Huawei Ascend NPU, to investigate the generalization ability of DARS on different models and hardware architectures. The experimental results are reported in Table 6, and

DARS improves the performance of the openPangu model consistently on all datasets.

As the results show, our method still outperforms the baseline in both the Pass@1 and Pass@K metrics.

*Table 5. Overall performance of Pass@1 (Avg@128) and Pass@128 of Qwen2.5-7B-Instruct.*

Model	AIME24	Math500	Olympiad	AMC	Minerva	Avg@128	Pass@128
Qwen2.5-7B-Instruct	11.9	72.3	37.1	42.2	31.9	47.2	80.3
GRPO-baseline	14.2	74.8	37.6	43.4	33.4	48.6	78.8
<b>DARS-HW-Breadth</b>	<b>15.6</b>	<b>76.5</b>	<b>38.4</b>	<b>44.7</b>	<b>34.6</b>	<b>49.6</b>	<b>82.3</b>

*Table 6. Overall performance of DARS with openPangu on Ascend NPU.*

Model	AIME24	Math500	Olympiad	AMC	Minerva	Avg@32	Pass@32
openPangu-7B	36.99	82.71	48.82	51.61	37.0	57.54	79.92
<b>openPangu-7B + DARS</b>	<b>60.58</b>	<b>93.95</b>	<b>67.96</b>	<b>81.06</b>	<b>43.4</b>	<b>72.56</b>	<b>86.59</b>

### E.7. Explanation of Significant Pass@k Gain for Llama-3

The stronger gains for Llama-3 likely stem from its base model characteristics. Recent studies (Gandhi et al., 2025; Wang et al., 2025) suggest that base models like Llama-3 lack mid-training, causing many valid responses to appear only at higher sampling budgets. As shown in the table below, Llama-3-8B-Base exhibits a much larger performance gap when increasing (K) from 8 to 32/64 compared to Qwen models as shown in Table 7. This indicates that Llama-3 has more correct solutions “hidden” deeper in the sampling space. Our DARS method, by focusing on hard examples, effectively uncovers these “deep” correct samples, leading to more substantial Pass@K improvements for Llama-3.

*Table 7. Pass@K gap comparison of Qwen2.5-Math-1.5/7B and LLama3-8B-Base*

Model	Pass@8	Pass@32 - Pass@8	Pass@64 - Pass@8
Qwen2.5-Math-1.5B	56.5	12.4	17.1
Qwen2.5-Math-7B	63.5	10.5	14.4
<b>Llama3-8B-Base</b>	<b>17.2</b>	<b>19.1</b>	<b>27.3</b>

### E.8. Thinking Length Dynamics

This section investigates how DARS influences the reasoning length of LLMs. We tracked the response length dynamics during the training of Qwen2.5-Math-1.5B and 7B models. Our experiments reveal two key observations: (1) The training process shows a clear trend of increasing generation length, as shown in Figure 15. (2) When evaluated on AIME 2024, models trained with DARS consistently produce longer reasoning traces than the baseline, as shown in Figure 16 (For steps in multiples of 100, we take the average of 128 sampling results. To increase the density of data points, we also sample 16 times for every intermediate 50-step interval and take the average). These results provide concrete evidence that our DARS method successfully stimulates the model to perform deeper and more thorough thinking.

## F. Discussion and Future Work

In this section, we analyze how hyperparameters  $N$  and  $N^{\max}$  control the shape of the cumulative advantage curve, and how this shape may influence training behavior. We further discuss how dynamically adjusting these parameters could enable a smooth transition from Pass@K-oriented to Pass@I-oriented training.

### F.1. Hyperparameter Control of Cumulative Advantage Shape

We show the Cumulative Advantage shape of ET/HW schedule with  $N = 8$  in Figure 17. By continuously reducing the size of  $N_{\max}$ , the curve will contract accordingly. When  $N_{\max} = N$ , it is equivalent to the vanilla method without DARS.

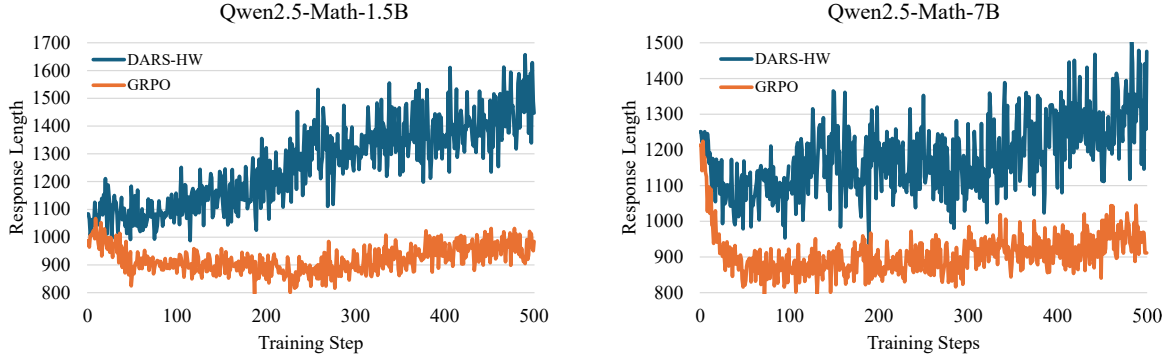


Figure 15. Training dynamics of response length for GRPO and DARS.

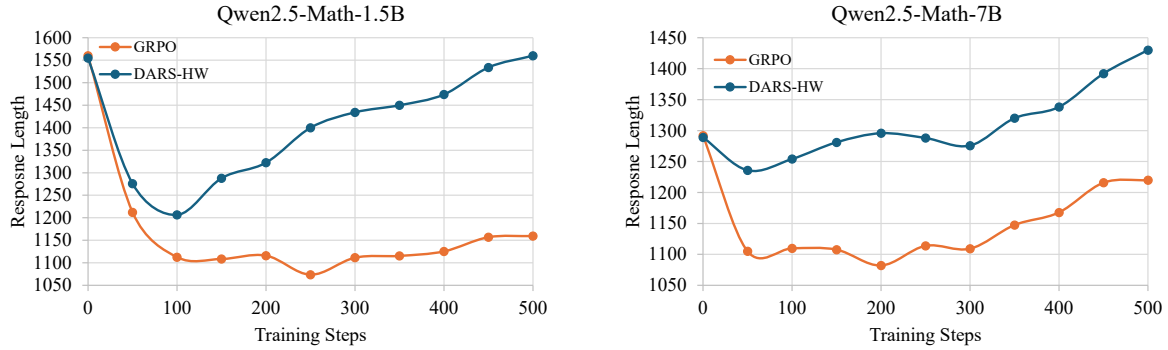


Figure 16. Statistical results of response length on AIME 2024 for GRPO and DARS.

## F.2. Potential Pass@K to Pass@1 Training Transition

The dynamic control of  $N^{\max}$  suggests an intriguing training strategy: starting with a large  $N^{\max}$  value to maximize  $Pass@K$  performance through extensive exploration of hard problems, then gradually reducing  $N^{\max}$  throughout training to transition toward  $Pass@1$  optimization. This approach mirrors curriculum learning principles, where the training difficulty is progressively adjusted. Initially, the model benefits from the expanded solution space and diverse reasoning patterns discovered through heavy sampling on hard problems (high  $N^{\max}$ ). As training progresses and the model’s capability matures, reducing  $N^{\max}$  focuses the training on refining the most promising solution strategies, ultimately improving single-shot performance. Future work will explore optimal annealing schedules for  $N^{\max}$  and investigate whether this transition strategy can simultaneously maximize both  $Pass@1$  and  $Pass@K$  performance, potentially overcoming the current limitations of RLVR training.

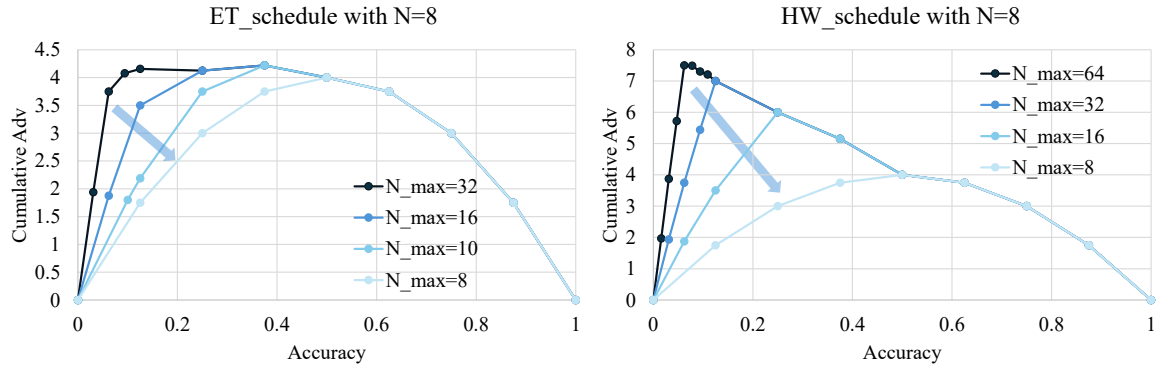


Figure 17. Control the shape of Cumulative Advantage by adjusting the  $N_{\max}$  hyperparameter of DARS.